^{31}P MRS of the brain supports the mitochondrial hypothesis for Huntington disease, revealing altered ATP synthesis, pH increase and stable ATP level

M. Chaumeil[1], H. Bataille[1], J. Valette[1], E. Brouillet[1], V. Gaura[1], A. C. Bachoud-Levi[2], P. Krystkowiak[3], C. Verny[4], P. Damier[5], A. Rialland[2], G. Bloch[1], P. Hantraye[1], P. Remy[1,2], and V. Lebon[1,6]

[1]CEA-CNRS, Orsay, France, [2]CHU Henri Mondor, Créteil, France, [3]CHRU Roger Salengro, Lille, France, [4]CHRU Larrey, Angers, France, [5]CHRU Guillaume et Rene Laënnec, Nantes, France, [6]CEA-NeuroSpin, Gif-sur-Yvette, France

Introduction

Huntington disease (HD) is a neurodegenerative disorder characterized by abnormal movements (chorea), dementia, and preferential degeneration of the striatum and to a lesser extent cerebral cortex. Mechanisms of neurodegeneration in HD remain unknown. One hypothesis is that mitochondrial defects may play a role in the pathogenesis of this disorder [1]. In this context, ^{31}P spectroscopy provides a potentially powerful technique for characterizing *in vivo* possible impairment in energy metabolism in HD. ^{31}P spectroscopy has been carried out in muscles of HD patients, suggesting peripheral defects in energy metabolism [2]. However, to our knowledge, this approach has never been applied for *in vivo* analysis of the brains of HD patients. In the present study, our main objective was to develop an acquisition method for brain ^{31}P spectroscopy applicable within a reasonable examination time (~30 min) on a clinical 3 Tesla system in order to directly assess brain energy metabolism in HD patients. Since our HD patients present whole-brain atrophy, a non-localized ^{31}P spectroscopy method was developed. Then the concentrations of ^{31}P cerebral metabolites, the flux of ATP synthesis (V_{ATP}) and the intracellular pH (pHi) were determined for HD patients and controls.

Materials & Methods

Subjects and NMR system ^{31}P NMR spectra were acquired from 9 HD patients presenting global brain atrophy (6 males, 3 females, aged 46±9) and 6 age- and sex-matched controls (4 males, 2 females, aged 42±8). Experiments were performed on a whole-body 3T Bruker system equipped with a quadrature birdcage coil resonating at 50.7MHz (^{31}P frequency). The edge of the cylindrical coil was positioned at the level of the upper lip so that the detection volume contained the brain while avoiding strong muscle contamination.

Pulse-Acquire ^{31}P Spectroscopy Fisrt order shimming was performed manually on the ^{31}P signal, leading to a ~15Hz line width on PCr. Spectra were then collected using a pulse-acquire ^{31}P sequence without localization (100µs 90° hard pulse, TR=7.5s, NT=28). The use of a non-localized approach resulted from the finding that skeletal muscle contamination was low: in order to asses muscle contamination, 3D gradient echo MRI was performed using a ^{1}H coil having the exact same geometry as our ^{31}P coil. Image segmentation showed that the detection volume contained the entire brain, while muscle accounted for only ~7% of detected tissue (data not shown).

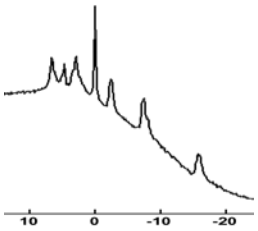

***Fig.1**. Pulse-acquire ^{31}P spectrum acquired in one volunteer.*

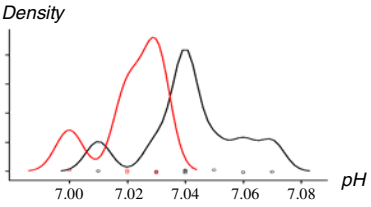

***Fig.2.** pH density plot for controls (**red**) and HD patients (**black**).*

Progressive Saturation Transfer Experiment A saturation broad pulse (length t_{sat}) was added just before the 90° hard pulse of the pulse-acquire ^{31}P sequence. The saturation frequency was first set to γ-ATP frequency and spectra were collected for 4 values of t_{sat} (0.25, 0.5, 1.0, 1.5s). TR was kept to 7.5s and NT to 28 for each t_{sat}. Control measurements were also collected for RF bleed over correction [3]. The total acquisition time was ~35minutes. According to primate studies at 3T [4], the longitudinal relaxation time $T1^{int}$ of Pi was expected to be 2.1s in the human brain. Thus a 7.5s repetition time allows Pi to achieve almost full relaxation (~98%) between 2 repetitions.

Spectra quantification ^{31}P spectra were quantified using an original basis set implemented for AMARES method in jMRUI [5]. Thirteen ^{31}P multiplets were described [6]. In order to get rid of the broad baseline signal, the FIDs were left-shifted 12 points (1.2ms) for quantification. Then the estimated resonances were corrected for amplitude and line widths taking into account the truncated points.

Evaluation of pHi For each subject, pHi was calculated with jMRUI from the chemical shift of Pi relative to PCr measured on pulse-acquire ^{31}P spectra [7]. The parameters of Pi-PCr system were set to pK=6.77, δ_{HA}=3.23ppm and δ_A=5.70ppm.

Determination of the rate of ATP synthesis V_{ATP} Pi attenuation was estimated for each volunteer and each saturation time and then averaged for controls and patients respectively. An iterative fitting of *Pi attenuation vs. t_{sat}* was performed for the 2 datasets, leading to an estimation of k_f and $T1^{int}$ parameters for each group. In order to stabilize the procedure, $T1^{int}$ was constrained around 2.1s ($1.7s<T1^{int}<2.5s$). Monte Carlo simulation was performed on this dataset in order to assess fit accuracy. ATP synthesis rate $V_{ATP}= k_f \times[Pi]$ was derived from k_f determination for each group.

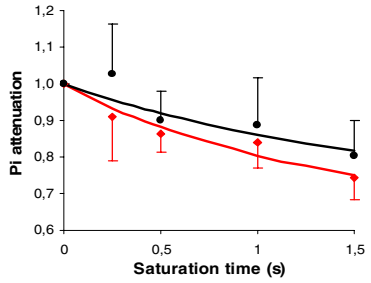

***Fig.3.** Pi attenuation vs. saturation time t_{sat}. For each group (controls in **red**, HD patients in **black**), solid lines are the best fit to experimental Pi attenuation (♦) (♦).*

Results and discussion

A typical ^{31}P spectrum is shown in Fig. 1. Estimations of metabolite relative contents for controls and HD patients are presented in Table 1. For each metabolite, the relative content was calculated as the ratio of metabolite peak area to the sum of all ^{31}P peak areas. As reported in this table, no significant difference can be noticed in metabolite concentrations between HD patients and controls.

^{31}P spectra analysis exhibits a higher value of pHi for the HD group than for controls (Table 1). Wilcoxon statistic analysis performed on the 2 datasets reveals that the observed pHi difference is significant (*p=0.02*) (Fig.2). This is the first report of significant increase in cerebral pHi in HD patients.

Iterative fitting of Pi attenuation (Fig. 3) yielded k_f^C=0.29±0.025s^{-1} and $T1^{intC}$=1.9±0.33s for controls, and k_f^{HD}=0.19±0.031s^{-1}, $T1^{intHD}$=2.3±0.34s for HD patients. Monte Carlo simulation shows that fitting Pi attenuation provides the same accuracy on $T1^{int}$ determination for both groups (~15%). However, accuracy on k_f is nearly two-times higher for controls (s.d. ~9%) than for HD patients (s.d. ~16%), illustrating the expected dispersion of Pi attenuation values in patients. Using a brain density of 1.1g/mL and [Pi]=1.2mM [6], the cerebral rate of ATP synthesis in controls and patients was V_{ATP}^C=19±2µmol.g^{-1}.min^{-1} and V_{ATP}^{HD}=12±2µmol.g^{-1}.min^{-1}, exhibiting a significant ~35% decrease in HD group.

The stability of metabolic pools (Table 1) reveals that ATP neuronal homeostasis is, at steady state, maintained in HD brains, even though the rate of ATP synthesis is reduced by ~35%. The reduction in V_{ATP} means that both ATP synthesis and degradation are lower in steady state in HD patients, consistent with possible mitochondrial defects. One important consequence of reduced V_{ATP} in HD might be that neurons would have reduced capacity to cope with energy demands associated with neuronal stimulation. Thus alteration of V_{ATP} could participate to neuronal dysfunction and eventually neurodegeneration. Finally, pHi increase is consistent with a reduced mitochondrial protonic gradient, and thus with a lower value of V_{ATP}. To conclude, our findings are in support of the mitochondrial hypothesis for HD.

	Metabolite Relative Content (u.a. , mean±s.d.)									pH	V_{ATP} (µmol.g^{-1}.min^{-1})
	α-ATP	β-ATP	γ-ATP	Pi	PCr	PME	PDE	MP	DN		
Controls (n=6)	0.127 ±0.009	0.101 ±0.006	0.108 ±0.002	0.069 ±0.002	0.160 ±0.009	0.123 ±0.006	0.138 ±0.013	0.115 ±0.027	0.035 ±0.06	7.022 ±0.012	18.98 ±1.64
Patients (n=9)	0.127 ±0.009	0.101 ±0.006	0.111 ±0.005	0.068 ±0.002	0.165 ±0.011	0.124 ±0.007	0.142 ±0.008	0.104 ±0.006	0.034 ±0.007	**7.048*** ±0.024	**12.44*** ±2.03

***Table 1.** ^{31}P metabolite contents. PME includes PE, PC and PSer. PDE includes GPE and GPC. (*) Values showing significant differences between controls and HD.*

1.Brouillet et al. , J. Neurochem., 95 :1521-40 (2005) **2**.Lodi et al. , Ann. Neurol. 48(1):72-6 (2000) **3**.Lei et al, Proc. Natl. Acad. Sci USA 100 :14409-14 (2003) **4**.Valette et al, ISMRM (2006) **5**.Naressi et al, Comput. Biol. Med., 31 :269-86 (2001) **6**.Jensen et al, NMR Biomed., 15 :338-47 (2002) **7**.Petroff et al, Lancet, 2 :105-6 (1983)